PHYSOR 2012 Advances in Reactor Physics Linking Research, Industry, and Education
Knoxville, Tennessee, USA, April 15-20, 2012, on CD-ROM, American Nuclear Society, LaGrange Park, IL (2012)

^{183}W RESONANCE PARAMETER EVALUATION IN THE NEUTRON ENERGY RANGE UP TO 5 KEV*

M. T. Pigni,† M. E. Dunn, K. H. Guber
Oak Ridge National Laboratory, Nuclear Data & Criticality Safety
Oak Ridge, TN, 37831-6170, USA
pignimt@ornl.gov; dunnme@ornl.gov; guberkh@ornl.gov

ABSTRACT

We generated a preliminary set of resonance parameters for ^{183}W in the neutron energy range of thermal up to 5 keV. In the analyzed energy range, this work represents a significant improvement over the current resonance evaluation in the ENDF/B-VII.1 library limited up to 2.2 keV. The evaluation methodology uses the Reich-Moore approximation to fit, with the R-matrix code SAMMY, the high-resolution measurements performed in 2007 at the GEel LINear Accelerator (GELINA) facility. The transmission data and the capture cross sections calculated with the set of resonance parameters are compared with the experimental values, and the average properties of the resonance parameters are discussed.

Key Words: Neutron cross section, Nuclear data, R-matrix theory

1. INTRODUCTION

Tungsten is a key structural material that can have significant impacts (i.e., in terms of neutron sensitivity) for nuclear applications such as shielding, fast breeder reactors, critical assemblies of fissionable materials, etc. It is also important for production of two unstable isotopes, ^{185}W ($t_{1/2} = 75.1$ d) and ^{187}W ($t_{1/2} = 23.7$ h), that may be used as radioactive tracers. Naturally occurring tungsten ^{nat}W consists of four stable isotopes, ^{182,183,184,186}W plus an extremely long half-life isotope, ^{180}W ($t_{1/2} = 1.8 \cdot 10^{18}$ y). The even-A stable isotopes have spin-parity $I^\pi = 0^+$ that couples to s-wave neutrons to make compound-nuclear states all characterized by the same spin-parity $J^\pi = 1/2^+$, whereas the only odd-A stable isotope, ^{183}W having $I^\pi = 1/2^-$, couples to make two compound-nuclear states $J^\pi = 0^-$ and $J^\pi = 1^-$. These isotopes occur in the mass region of the split $4s$ giant resonance in the S_0 strength function where the p strength function S_1 is appreciably smaller than S_0. With an appropriate sample thickness, this highly enhances the probability that the measured resonances belong to a pure single population of s levels because most or all s levels are measured, including only few if any p levels.

In view of the interest in tungsten metal for several distinct types of nuclear applications, it is important to have a thorough understanding of its interaction with neutrons. The evaluation of the ^{183}W neutron-resonance parameters in the ENDF/B-VII.0 library was performed in the seventies

*Notice: This manuscript has been authored by UT-Battelle, LLC, under contract DE-AC05-00OR22725 with the U.S. Department of Energy. The United States Government retains and the publisher, by accepting the article for publication, acknowledges that the United States Government retains a non-exclusive, paid-up, irrevocable, world-wide license to publish or reproduce the published form of this manuscript, or allow others to do so, for United States Government purposes. The U.S. Department of Energy Nuclear Criticality Safety Program sponsored the preparation of this paper.

†Corresponding author

for the ENDF/B-V library and successively adopted by the different releases of ENDF. The evaluation was based on the analysis of resonance parameters performed by Goldberg et al. [1] along with the results of capture and transmission measurements performed by Bartolome et al. [2] over the energy range from thermal up to 760 eV. Those measurements had poor energy resolution but had higher-level detection sensitivity. Consequently, many very weak p-wave or spurious levels were included and might have led to unrealistic s-wave data. In the ENDF/B-VII.1 library that is to be released, the ^{183}W evaluation in the resolved resonance region is extended to 2.2 keV. This evaluation, based on the JENDL-3.3 library with small adjustments to the parameters by Leal, uses the results of neutron time-of-flight resonance measurements performed by Camarda et al. [3] and Ohkubo [4] in the early seventies, and by Macklin et al. [5] in the eighties, along with the values of resonance parameters taken from the work of Mughabghab [6].

Following the series of recent measurements on the stable isotopes of tungsten performed at the GEel LINear Accelerator (GELINA) by Lampoudis et al. [7], the aim of the present work is to evaluate a new set of neutron resonance parameters for total and capture cross sections on ^{183}W in the energy range of thermal energy up to 5 keV. The analysis of the experimental data of Lampoudis et al. uses the code SAMMY [8], which performs a multi-level multi-channel R-matrix fit to neutron data in the Reich-Moore formalism. Experimental conditions such as resolution function, finite size sample, nonuniform thickness, and nuclide abundances of sample, multiple scattering, self-shielding, normalization, background, and Doppler broadening are taken into account. From both the capture and transmission data we were able to determine pertinent resonance parameters; and from these, the values of their systematics, such as strength functions, level spacings, and cumulative plots. In thermal energy range, we utilized the recently published *Atlas of Neutron Resonances* [9] as well as the tabulated neutron scattering lengths [10] as a source of information on scattering and capture cross-sections, and resonance integral.

The paper is organized as follows. The evaluation methodology is outlined in Section 2; the calculations and results are presented and discussed in Section 3 and followed by our conclusions in Section 4.

2. METHODOLOGY

Our methodology is based on the SAMMY code system, which is a modern tool for calculating neutron cross sections mainly used for nuclear data evaluations in the resolved resonance region (RRR). The code incorporates selected R-matrix approximations coupled to the Bayesian method in order to fit experimental data and ultimately to generate a set of resonance parameters with related covariance matrix. For this task we based our results on the Reich-Moore formalism, which approximates the expression for elastic and reaction cross sections better than other single- and multi-level variants of the R-matrix theory.

2.1. The Exact R-Matrix Expression

Resolved resonances are described most conveniently by R-matrix theory, which attains its standard form with the article of Lane and Thomas [11] in which a comprehensive derivation of the equations can be found. Here, we define the quantities that are relevant to the discussion of this work, using a notation similar to that one found in Fröhner's report [12]. The angle-integrated

cross section $\sigma_{cc'}$ of the exit channel c', with associated quantum numbers $J\ell' s'$ induced by the interaction between the target and the projectile in the entrance channel c with quantum number $J\ell s$, is given as

$$\sigma_{cc'} = \frac{\pi}{k_c^2} \sum_J g_J \sum_{\ell\ell'} \sum_{ss'} |\delta_{cc'}\delta_{\ell\ell'}\delta_{ss'} - U^J_{c\ell s,\, c'\ell' s'}|^2 \,, \tag{1}$$

where the spin statistical factor for given spins of the two collision partners i and I is

$$g_J = \frac{2J+1}{(2i+1)(2I+1)} \tag{2}$$

and the collision matrix U can be expressed in terms of the level matrix A as

$$U^J_{c\ell s,\, c'\ell' s'} = e^{-\imath(\phi_\ell + \phi_{\ell'})} \big(\delta_{cc'}\delta_{\ell\ell'}\delta_{ss'} + \imath \sum_{\lambda\mu} \sqrt{\Gamma^{J,\lambda}_{c\ell s}} A_{\lambda\mu} \sqrt{\Gamma^{J,\mu}_{c'\ell' s'}}\big) \,, \tag{3}$$

$$\sqrt{\Gamma^{J,\lambda}_{c\ell s}} = \gamma^{J,\lambda}_{c\ell s} \sqrt{2P_\ell} \,, \tag{4}$$

$$(\mathbf{A}^{-1})_{\lambda\mu} = (E_\lambda - E)\delta_{\lambda\mu} - \sum_c \gamma^{J,\lambda}_{c\ell s}(S_\ell + \imath P_\ell - B_\ell)\gamma^{J,\mu}_{c\ell s} \,. \tag{5}$$

One can show that the relationship between the level matrix $\mathbf{A}$ and the channel matrix $\mathbf{R}$ is given by

$$\sum_{\lambda\mu} \gamma^{J,\lambda}_{c\ell s} A_{\lambda\mu} \gamma^{J,\mu}_{c'\ell' s'} = \sum_{c''} (\mathbb{I} - RL)^{-1}_{c\ell s, c''\ell' s'} R^J_{c''\ell s, c'\ell' s'} \,,$$

$$(\mathbb{I} - RL)_{c\ell s, c'\ell' s'} \equiv \delta_{cc'}\delta_{\ell\ell'}\delta_{ss'} - \sum_{c''} R^J_{c\ell s, c''\ell' s'}(S_\ell + \imath P_\ell - B_\ell)\delta_{c''c'} \,,$$

where $\mathbb{I}$ is the identity matrix and the elements of the channel matrix $\mathbf{R}$ are

$$R^J_{c\ell s, c'\ell' s'} = \sum_{\lambda=1}^{\infty} \frac{\gamma^{J,\lambda}_{c\ell s}\, \gamma^{J,\lambda}_{c'\ell' s'}}{E_\lambda - E} \,. \tag{6}$$

In this notation each partition is fully specified by the total angular momentum J and the channel spin s obtained by the quantum-mechanical triangle relations $|\ell - s| \le J \le \ell + s$ and $|I - i| \le s \le I + i$, respectively. The quantum numbers s and s' define the spins of the incoming and outgoing pair of particles, respectively. The quantum number ℓ refers to the orbital angular momentum of the ℓ-th partial wave for the channel c. The relevant physical quantities in these equations are the partial width amplitudes $\Gamma^{J,\lambda}_{c\ell s}$ for the decay of compound state λ with level energy E_λ via the channel c. Hard-sphere phases ϕ_ℓ and logarithmic derivatives $L_\ell = S_\ell + \imath P_\ell$ depend on the incoming and outgoing radial wave functions, $I_\ell \equiv I_\ell(r_c; k_c)$ and $O_\ell \equiv O_\ell(r_c; k_c)$, calculated at the channel radius a_c ,

$$\phi_\ell = \left[\tan^{-1} \frac{\mathrm{Im}\, O_\ell}{\mathrm{Re}\, O_\ell}\right]_{r_c = a_c} \quad \text{and} \quad L_\ell = \left[r_c \frac{\partial \ln O_\ell}{\partial r_c}\right]_{r_c = a_c} \tag{7}$$

which, for neutral projectiles, are proportional to the spherical Hankel functions of the first kind $O_\ell \equiv I^*_\ell = \imath k_c r_c h^{(1)}_\ell(k_c r_c)$ where the wave number $k_c = \sqrt{2M_c E_c}/\hbar$ relates the energy of relative

motion of the particles E_c and their reduced mass M_c. The $S_\ell = \mathrm{Re}\, L_\ell$ are called shift factors and $P_\ell = \mathrm{Im}\, L_\ell$ are centrifugal-barrier penetrabilities. These quantities describe the configuration space of the external region where nuclear forces are considered negligible. The internal region where the nuclear interaction becomes predominant is described by the logarithmic derivatives $B_\ell \equiv B_\ell(a_c; k_c)$ of the radial wavefunctions calculated at the channel radius a_c.

2.2. The Reich-Moore Approximation

The exclusion of the γ channel from the sum in Eq. (5),

$$(\mathbf{A}^{-1})_{\lambda\mu} = (E_\lambda - E - \bar{\Gamma}_{\lambda\gamma})\delta_{\lambda\mu} - \sum_c \gamma^{J,\lambda}_{c\notin\gamma\ell s}(S_\ell + \imath P_\ell - B_\ell)\gamma^{J,\mu}_{c\notin\gamma\ell s}\,, \tag{8}$$

is also known as Reich-Moore approximation. It derives from the observation that the diagonal elements of the level matrix have the same sign, whereas the off-diagonals decay amplitudes have random signs and comparable magnitudes. Therefore, if the diagonal elements all add up, the off-diagonal ones have the tendency to cancel out in the summation. The inversion of the level matrix $(\mathbf{A}^{-1})_{\lambda\mu}$ of Eq. (8) is equivalent to an eigenvalue problem with matrix

$$R^J_{c\ell s, c'\ell' s'} = \sum_{\lambda=1}^{\infty} \frac{\gamma^{J,\lambda}_{c\ell s}\gamma^{J,\lambda}_{c'\ell' s'}}{E_\lambda - E - \imath\bar{\Gamma}_{\lambda\gamma}/2}\,, \tag{9}$$

with E_λ in Eq. (8) replaced by $E_\lambda - \imath\bar{\Gamma}_{\lambda\gamma}/2$ and $\bar{\Gamma}_{\lambda\gamma} = \sum_{c\in\gamma}\Gamma^{J,\lambda}_{c\ell s}$. This matrix is also called a reduced matrix since it is defined for channels $c, c' \notin \gamma$.

One of the first steps in a resonance evaluation is to take into account the levels below and above the energy range of the resonance parameterization work. The enormous number of levels out of the analyzed energy range can be generally accounted for by the distant-level parameter $\mathcal{R}^{J,\infty}_{c\ell s}$ and a function $f(E; \boldsymbol{s}_c)$ of the neutron energy and a set of adjustable parameters $\boldsymbol{s}_c$. These quantities are defined by writing the reduced matrix in Eq. (9) as a sum of N known (or internal) levels and unknown (or external) levels as

$$R^J_{c\ell s, c'\ell' s'} = \mathcal{R}^J_{c\ell s, c'\ell' s'} + \sum_{\lambda=1}^{N} \frac{\gamma^{J,\lambda}_{c\ell s}\gamma^{J,\lambda}_{c'\ell' s'}}{E_\lambda - E - \imath\bar{\Gamma}_{\lambda\gamma}/2}\,, \tag{10}$$

where

$$\mathcal{R}^J_{c\ell s, c'\ell' s'} = [\mathcal{R}^{J,\infty}_{c\ell s} + f(E; \boldsymbol{s}_c)]\delta_{cc'}\,. \tag{11}$$

Figure 1 shows the total cross section of n+^{183}W (red continuous line) at incident energies between 0 and 5 keV. The cross sections are the sum of two contributions. The first contribution is the potential scattering cross section which, for s-waves, is given by

$$\sigma_{\text{pot}} = 4\pi a_c^2 \sum_J g_J (1 - \mathcal{R}^{J,\infty}_c)^2\,, \tag{12}$$

where the effective scattering radius is defined by the product of the channel radius a_c, and the distant-level parameter $\mathcal{R}^{J,\infty}_c$. In this work, the distant-level parameter was kept equal to zero and the channel radius was set to 7.3 fm. The second contribution is due to a multitude of external

levels below ($E < 0$) and above ($E > 5$ keV) the RRR, which are modeled by the following set of parameters

$$\begin{aligned}
E &= -965.0 \text{ eV}, \quad \Gamma_\gamma^0 = 90 \text{ meV}, \quad \Gamma_\text{n}^0 = 43.2 \text{ keV}, \\
E &= -33.08 \text{ eV}, \quad \Gamma_\gamma^1 = 90 \text{ meV}, \quad \Gamma_\text{n}^1 = 0.23 \text{ keV}, \\
E &= 5.025 \text{ keV}, \quad \Gamma_\gamma^1 = 90 \text{ meV}, \quad \Gamma_\text{n}^1 = 4.43 \text{ keV}, \\
E &= 5.077 \text{ keV}, \quad \Gamma_\gamma^1 = 90 \text{ meV}, \quad \Gamma_\text{n}^1 = 0.27 \text{ keV}, \\
E &= 5.796 \text{ keV}, \quad \Gamma_\gamma^1 = 90 \text{ meV}, \quad \Gamma_\text{n}^1 = 39.5 \text{ keV}.
\end{aligned}$$

These are the parameters $\boldsymbol{s}_c$ in Eq. (11), and their values were obtained by fitting to the cross sections computed by extrapolating the known RRR levels, and 2 bound, (i.e., negative) energy levels below and 3 levels above the 5 keV upper limit.

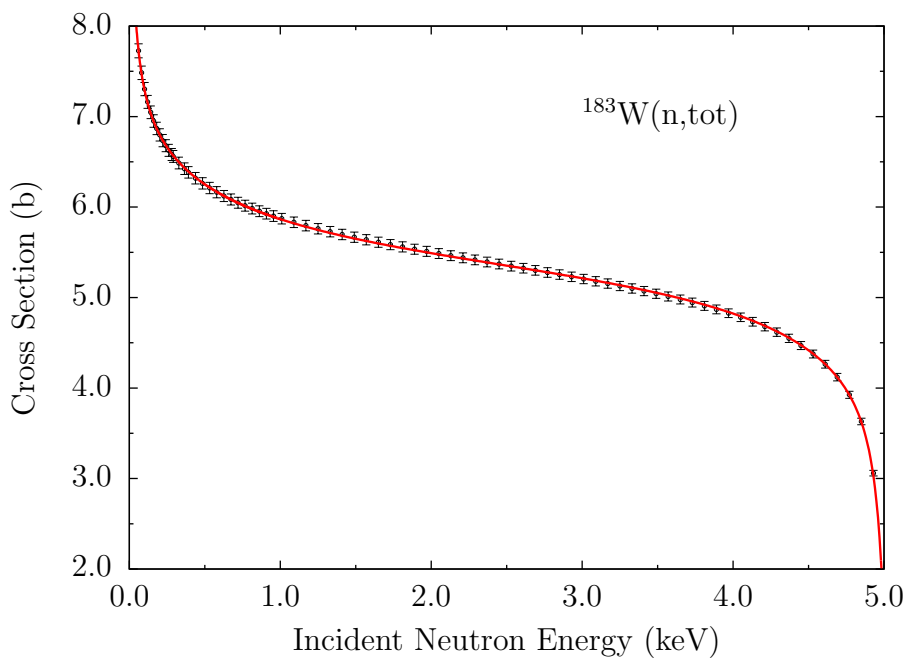

Figure 1. The potential scattering cross section calculated for a channel radius $a_c = 7.3$ fm and a distant-level parameter $\mathcal{R}_c^{J,\infty} = 0$ plus the contribution of 2 bound, i.e., negative levels below and 3 levels above the RRR 5 keV upper limit. The continuous red curve is a fit to the cross sections obtained by extrapolating the known RRR levels below and above the RRR.

Another important step in the evaluation procedure is to establish the number of partial waves that should be used in the fitting of the reduced-width amplitudes. Figure 2 graphs the hard-sphere penetrability factors of n+^{183}W for different partial waves $\ell = 0 - 4$ calculated at the channel radius $a_c = 7.3$ fm. As expressed in Eq. (5), the partial widths $\Gamma_{c\ell s}^{J,\lambda}$ are proportional to the product of the reduced-width amplitudes $\gamma_{c\ell s}^{J,\lambda}$, independent from the incident energy, and the penetrability factors P_ℓ. The magnitude of the latter determines the strength of the partial-

wave components responsible for the quasi-stationary compound state. Not unexpectedly, at low energies the magnitude of the penetrability factors is $\sim k_c^{2\ell+1}$. Penetrabilities become comparable in magnitude at about 2–3 MeV, where several partial waves are equally involved in the reaction mechanism. In this preliminary evaluation, we decided to neglect partial waves different from zero since the strength of the penetrability factors for $\ell > 0$ at energies of up to 5 keV was small, e.g., $P_1/P_0 \approx 10^{-5}$ at about 5 keV.

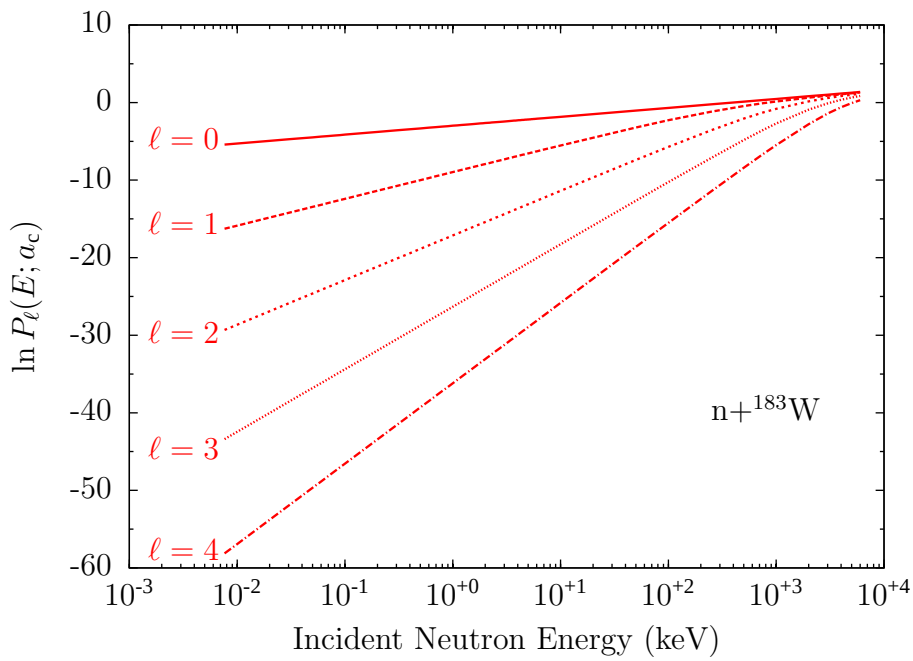

Figure 2. Hard-sphere penetrability factors $P_\ell \equiv P_\ell(E; a_c)$ of n+^{183}W for different angular momentum ℓ calculated at the channel radius $a_c = 7.3$ fm.

3. RESULTS AND SYSTEMATICS

3.1. The Thermal Region

The preliminary results of the SAMMY fit at thermal energy are displayed for ^{183}W(n,tot) in Fig. 3. For capture cross sections, the results are based on the value found in the *Atlas of Neutron Resonances*. However, for the scattering cross sections we believe that the value found in the Atlas is underestimated and we relied on the value of scattering cross sections found in the tables of reference [10]. This is also supported by the precise value of the bound coherent scattering length $b_{\text{coh}} = 6.59 \pm 0.04$ fm [9] [10]. We believe that the origin of the underestimated value of the scattering cross section, i.e. $\sigma_{\text{scat}} = 2.4$ b, derives from the measurement of the coherent scattering length reported by Alenxandrov et al. [13]. The solid red line represents the cross sections calculated by the resonance parameters, and it is compared with ENDF/B-VII.0 (in green) and JENDL-4 (in blue) nuclear data libraries. We noticed that the JENDL-4 evaluation follows the Atlas prescription,

whereas the evaluation in ENDF-B-VII.0 library overestimates the Atlas thermal value by about 4.5%. The preliminary values of thermal cross sections calculated at 0.0253 eV are also given in Table I. These values can be adjusted by small variations of the parameters of the resonance at negative energies such as those given in Section 2.

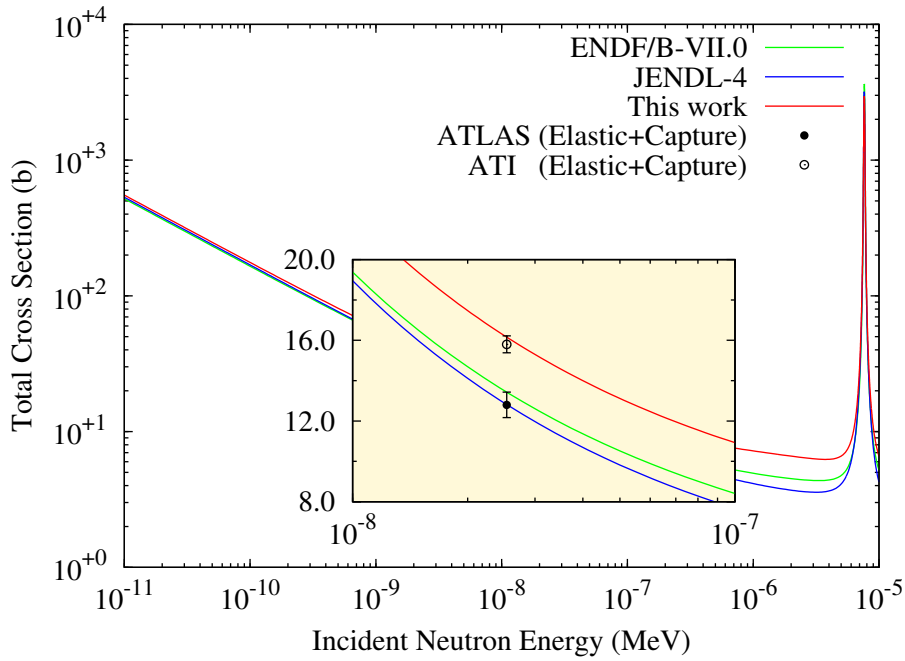

Figure 3. Total cross sections of ^{183}W compared with ENDF/B-VII.0 and JENDL-4 nuclear data libraries.

Table I. Thermal cross sections compared with the values of two major libraries, *Atlas of Neutron Resonances*, and the tabulated values of reference [10].

Thermal Cross Sections	Total (b)	Capture (b)	Elastic (b)
This work	16.140	10.520	5.620
ATI	—	10.100	5.700
JENDL-4	12.815	10.406	2.409
ENDF/B-VII.0	13.427	10.010	3.417
ATLAS	—	10.400	2.400

3.2. The Resolved Resonance Region

A preliminary set of parameters for 339 resonances is obtained in the energy range between thermal and 5 keV. The values of resonance parameters are derived from the sequential fit of transmission data and capture cross sections measured by Lampoudis et al. [7]. The calculated cross sections for total, elastic, and capture reaction channel are based on the R-matrix code SAMMY, in which the Reich-Moore approximation was adopted. In the fitting procedure, we also took into account the isotopic composition of the sample used in the measurements. Altogether, four isotopes of tungsten with the isotopic compositions ^{182}W (6.44%), ^{183}W (80.9%), ^{184}W (9.52%), and ^{186}W (3.14%) were simultaneously considered in the SAMMY regression calculations. For the resolution function related to the experimental facility, we used the GELINA parameterization taken from Ref. [8].

In Figs. 4–7 the calculated capture cross sections and transmission data (in continuous red lines) are compared with the experimental data. The values of the spin J for each resonance related to ^{183}W are also shown (in blue). When not reported, we considered the resonance belonging to one of the tungsten isotopes mentioned above. In Figs. 4–7 we note that in the energy region of 2.5–3.25 keV, one of the filters used in the measurements of transmission data (namely to determine the level of background from the sample holder or the scattered neutrons) generated inconsistent experimental data. Therefore, a meaningful fitting of the data in this energy region is temporarily not possible. We aim to resolve the problem using a different set of experimental data and/or new measurements by Lampoudis. The overall agreement of our results with Lampoudis's measurements is exceptionally good in the energy range up to 2.5 keV where the resolution of experimental data is pretty high. Above 2.5 keV, although the resolution of the resonances worsens, we were able to obtain a reasonable agreement in line with the scope of this preliminary analysis.

3.3. The Systematics of Resonance Parameters

In addition to presenting our results for the observed neutron resonance energies, E, neutron widths, $\Gamma_{\rm n}^J$, and capture widths, Γ_γ^J, we report the preliminary results for the systematics of the observed s-wave resonances, such as level spacing systematics and strength functions.

Figure 8 shows the cumulative number of observed resonance N versus the incident neutron energy E for ^{183}W. The figure shows a nearly linear slope that extends to about 5 keV. This indicates that in the vast majority of our reported levels, there are no missed narrow weak s-levels. The figure includes various fitted straight lines, which imply mean s-level spacings $\langle D_0^J \rangle$ for partial (red dashed lines) and mixed populations (solid red line). The $\langle D_0^J \rangle$ of ^{183}W tends to be much smaller than that of even-A isotopes, since ^{183}W has two randomly mixed independent populations with $J^\pi = 0^-$ and $J^\pi = 1^-$. Figure 8 also compares the recommended value taken from Mughabghab [9], which encompasses our value within 2.5 times its predicted uncertainty. The total number of observed levels up to 5 keV is $N = 339$, where about 70% of the levels (fractional density $f_0^1 = 0.706$) were selected with spin $J = 1$, which slightly exceeds the $2J + 1$ rule. The value $\langle D_0^J \rangle = 14.8$ eV, simply obtained by the ratio between the energy range (7 eV–5 keV) and $N - 1 = 338$ resonances, slighlty deviates from $\langle D_0^J \rangle = 14.4$ eV, obtained by the best fit of the cumulative number of observed levels (black dots).

Figure 9 graphs the cumulative reduced neutron widths, $\sum_m \Gamma_m^0$ related to the neutron width by

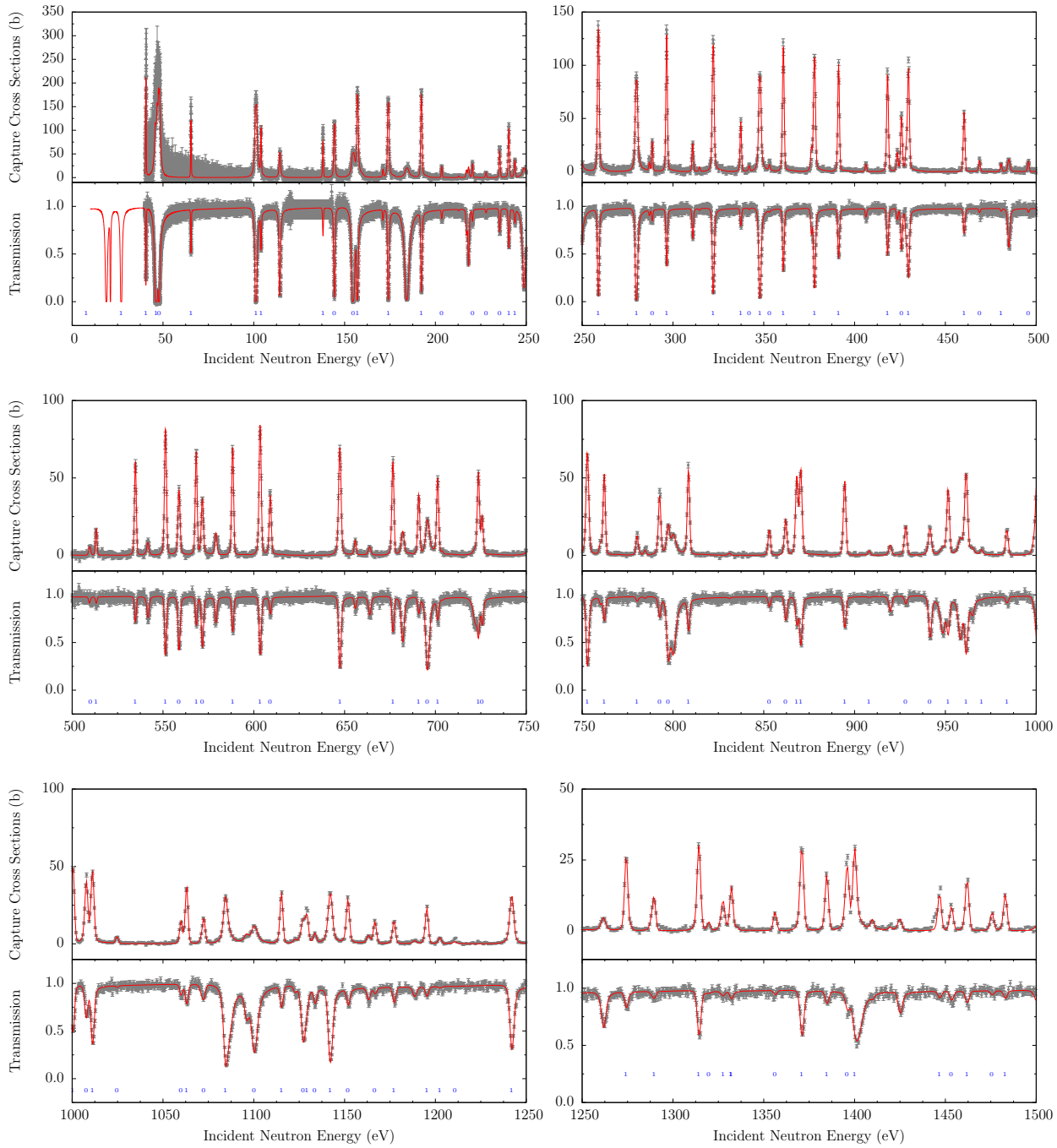

Figure 4. Neutron capture cross sections (top) and transmission data (bottom) of ^{183}W in the energy range of 10 eV to 1.5 keV. The solid red lines calculated by the resonance parameters are compared with the experimental data of Lampoudis et al. [7]. The value of the spin J is also shown for each level belonging to ^{183}W.

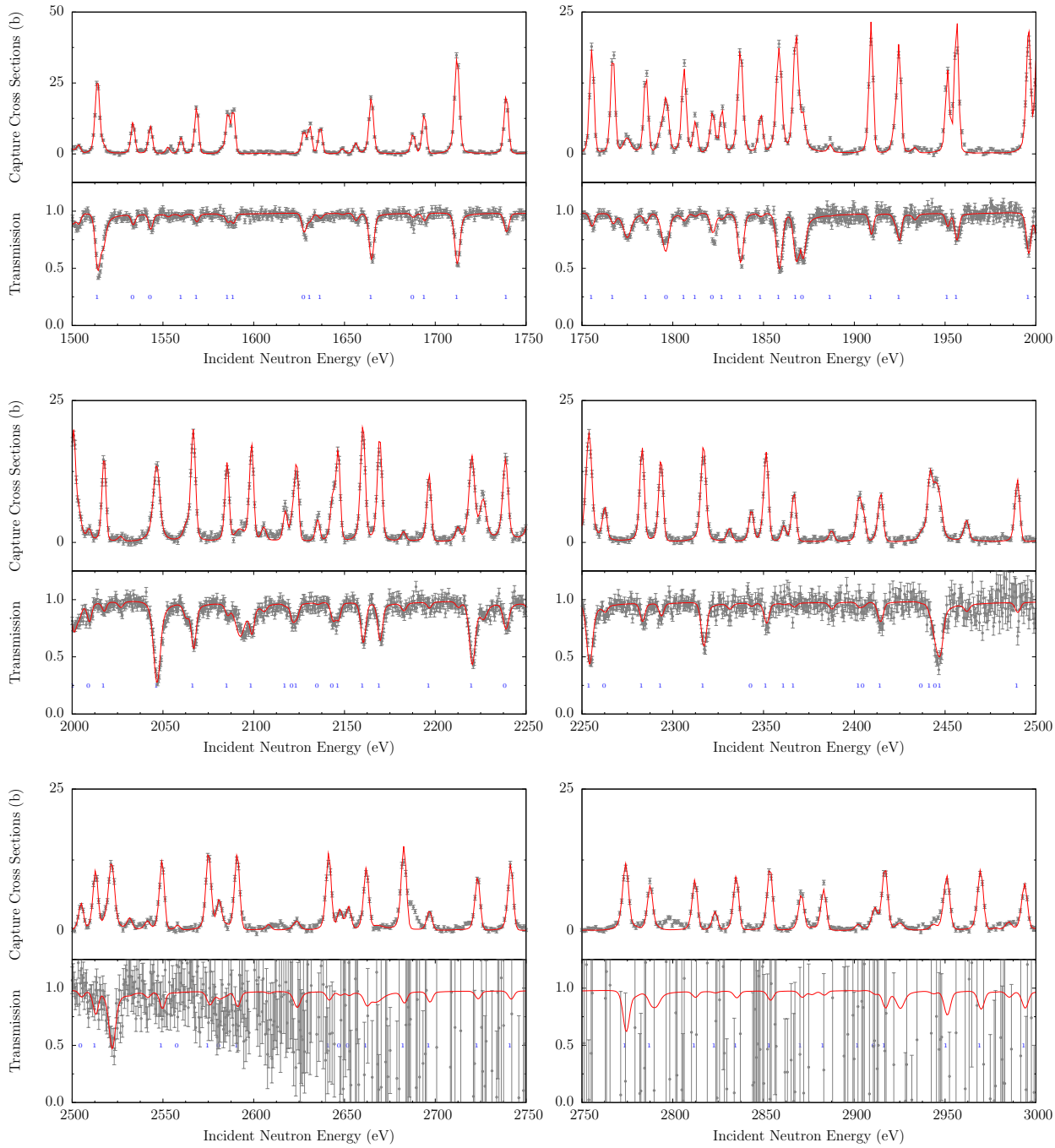

Figure 5. Neutron capture cross sections (top) and transmission data (bottom) of ^{183}W in the energy range of 1.5–3 keV. The solid red lines calculated by the resonance parameters are compared with the experimental data of Lampoudis et al. [7]. The value of the spin J (in blue) is also shown for each level belonging to ^{183}W.

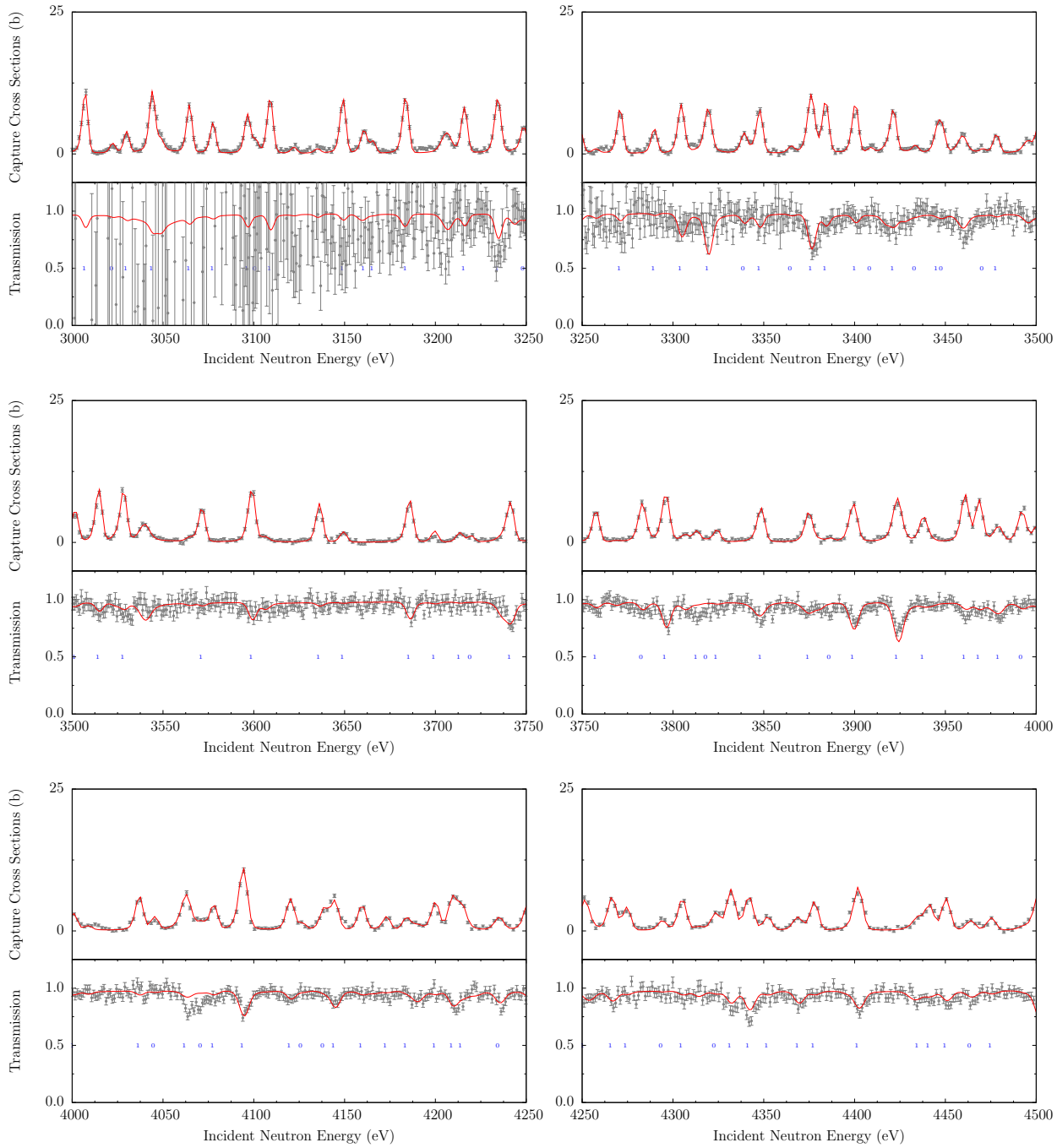

Figure 6. Neutron capture cross sections (top) and transmission data (bottom) of ^{183}W in the energy range of 3–4.5 keV. The solid red lines calculated by the resonance parameters are compared with the experimental data of Lampoudis et al. [7]. The value of the spin J (in blue) is also shown for each level belonging to ^{183}W.

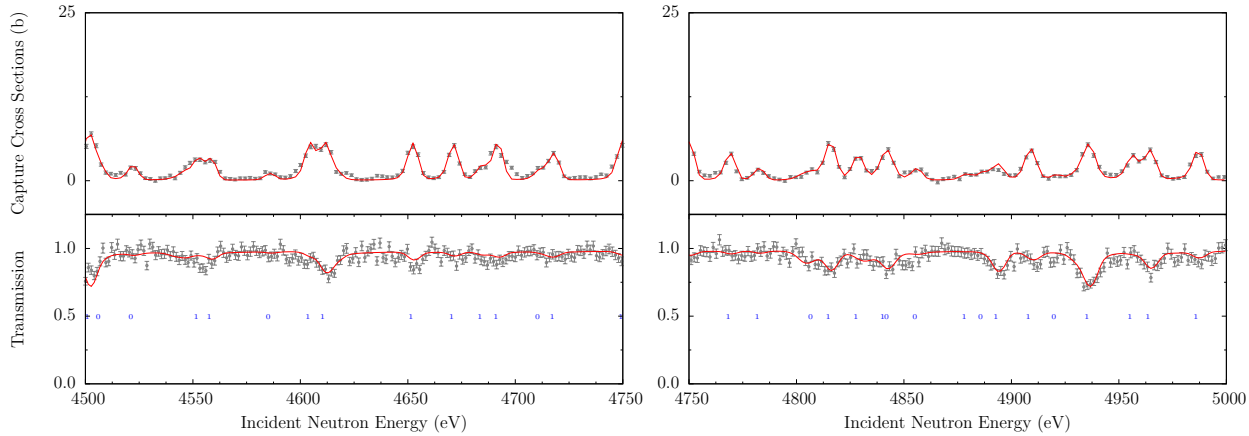

Figure 7. Neutron capture cross sections (top) and transmission data (bottom) of ^{183}W in the energy range of 4.5–5 keV. The solid red lines calculated by the resonance parameters are compared with the experimental data of Lampoudis et al. [7]. The value of the spin J is also shown for each level belonging to ^{183}W.

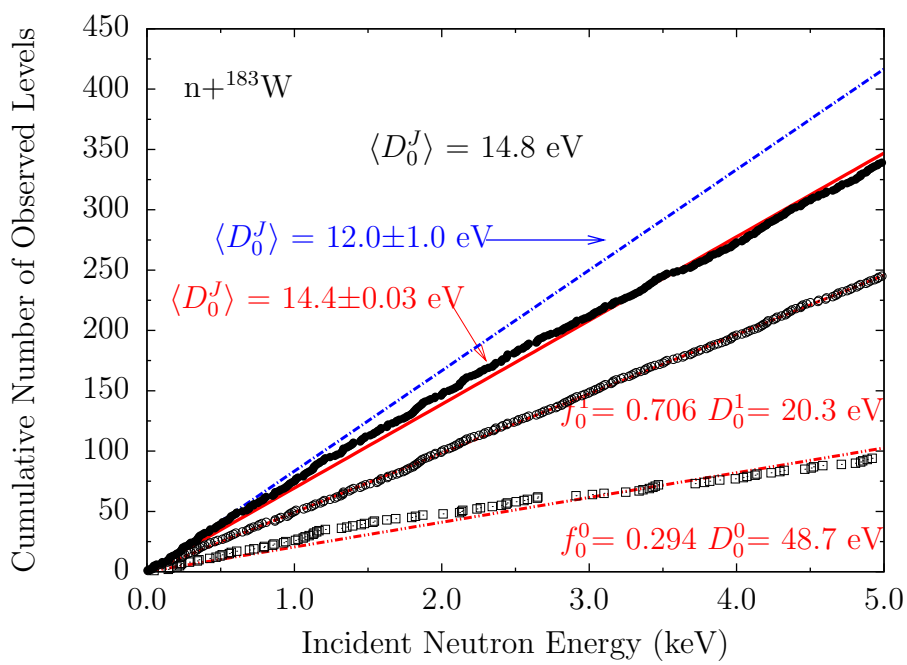

Figure 8. Plot of the cumulative number of observed s-levels (black dots) vs energy for n+^{183}W. The values of average s-level spacings for two J-spin populations, $\langle D_\ell^J \rangle$, and the mixed population, $\langle D_0^J \rangle$, shown in the plot represent the inverse of the slope of a straight line fitted to the data (red lines) and obtained by the recommended value (dashed blue line) taken from Mughabghab [9]. The expressions f_0^0 and f_0^1 are the fractional densities of population for $J^\pi = 0^-$ and $J^\pi = 1^-$, respectively.

$\Gamma^0_m = g_J \Gamma^{J,m}_{\rm n} \sqrt{1\ {\rm eV}/E_m}$. The slope of the plot obtained by the best fit of the reduced neutron widths (open dots) corresponds to the S_0 strength function and shows a deviation of about 5% with respect to the recommended value of Mughabghab [9]. We remark that a comprehensive analysis of the systematics of observed s-wave resonances should also include comparisons with known Gaussian Orthogonal Ensemble (GOE) distribution, e.g., comparison of the distribution of reduced widths done within the Porter-Thomas distribution.

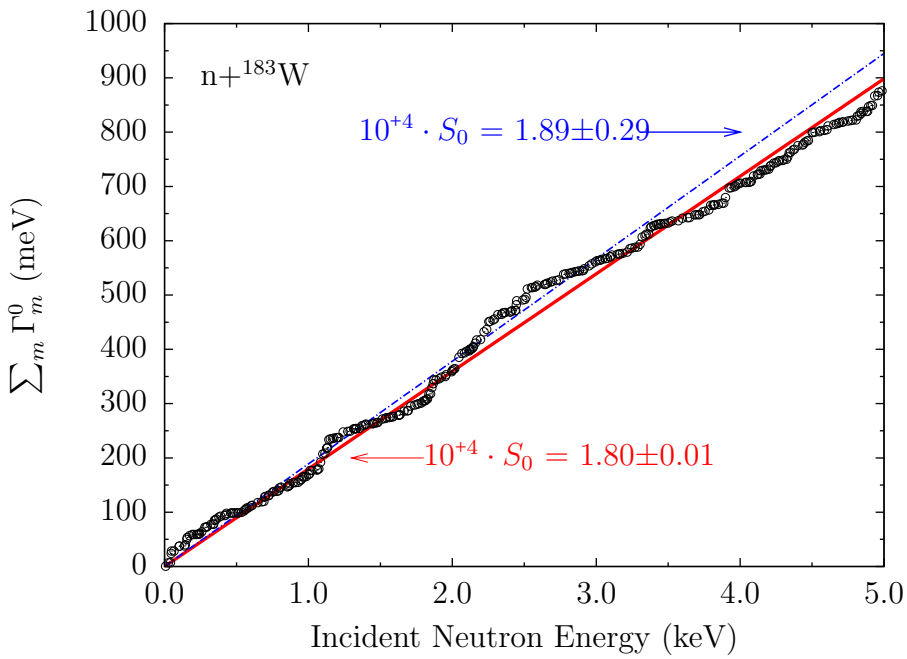

Figure 9. Plot of cumulative reduced neutron-widths $\sum_m \Gamma^0_m$ (open black dots) vs energy for n+^{183}W. The slopes of the straight lines give the strength function S_0 (in 10^{+4} unit). The slope of straight line fitted to the data (continuous red line) and the recommended value taken from Mughabghab [9] (dashed blue line) are shown.

4. CONCLUSIONS

We have applied the R-matrix SAMMY method using the Reich-Moore approximation to determine a consistent, albeit still preliminary, set of neutron resonance parameters for ^{183}W in the energy range up to 5 keV. In the analyzed energy range, this evaluation doubles the RRR energy range present in the latest US nuclear data library (ENDF/B-VII.1). These results are based on recent transmission and capture measurements of tungsten isotopes performed at GELINA. In the fitting of the resonance parameters, the experimental data were used sequentially to ensure that the calculated cross sections were in good agreement for both (n,tot) and (n,γ) reaction channel. However, the use of filters (used in the measurements to determine the level of background, for instance, from the sample holder and the scattered neutrons) caused difficulties in the analysis of resonance parameters in the energy range between 2.5 and 3.25 keV, as shown in Figs 5-6. We aim

to resolve this problem using a different set of experimental data or new measurements.

In the future we want to finalize this evaluation of resonance parameters and improve the analysis of their systematics. This would allow a statistical representation of the external function and a more precise determination of the level-distant parameter. A natural step would be also to include additional sets of experimental data in order to generate consistent assessments of cross section covariance data. We also intend to use the set of resonance parameters converted to ENDF/B format for nuclear criticality safety applications.

ACKNOWLEDGEMENTS

This work was supported by the US Nuclear Criticality Safety Program (NCSP) under contract No. DE-AC05-00OR22725 with UT-Battelle, LLC.

REFERENCES

[1] M. Goldberg et al., BNL-325 Report Supl. 2, Brookhaven National Laboratory, Upton, NY (1996).

[2] Z. M. Bartolome et al., "Neutron Radiative Capture and Transmission Measurements of W and Zr Isotopes in the keV Region," *Nucl. Sci. Eng.* **37**, p. 137 (1969).

[3] H. S. Camarda et al., "Neutron Resonance Spectroscopy. XII. The Separated Isotopes of W ," *Phys. Rev.* C**8**, p. 1813 (1973).

[4] M. Ohkubo, JAERI-M 5624 (1974).

[5] R. L. Macklin et al., *Neutron-Capture Cross Sections of the Tungsten Isotopes* ^{182}*W,* ^{183}*W,* ^{184}*W, and* ^{186}*W from 2.6 to 2000 keV*, LA-9200-MS (1982).

[6] S. F. Mughabghab, *Neutron Cross Sections*, Vol. 1, Part B (1984).

[7] C. Lampoudis, K. Guber, S. Kopecky, et al., "Neutron Total and Capture Cross Section of Tungsten Isotopes," ND2010: International Conference on Nuclear Data for Science and Technology, Jeju Island, Korea (2010).

[8] N. M. Larson, *Updated Users Guide for SAMMY: Multilevel R-Matrix Fits to Neutron Data Using Bayes Equations*, Report ENDF-364 and ORNL/TM-9179/R6, Oak Ridge National Laboratory, Oak Ridge, TN (May 2003). Also report ORNL/TM-9179/R7 (2006).

[9] S. F. Mughabghab, *Atlas of Neutron Resonances: Thermal Cross Sections and Resonance Parameters*, Elsevier Publisher, Amsterdam (2006).

[10] Neutron Scattering Lengths found at http://www.ati.ac.at/~neutropt/scattering/table.html.

[11] A. M. Lane and R. G. Thomas, "R-Matrix Theory of Nuclear Reaction," *Rev. Mod. Phys.* **30**, p. 257 (1958).

[12] F. H. Fröhner, *Evaluation and Analysis of Nuclear Resonance Data*, JEFF Report 18 (2000).

[13] Yu. A. Alexandrov, A. M. Balagurov, E. Maliszewsky, et al., *Yadernaya Fizika* **10**, p. 328 (1969).